COMPARISON OF CRATER RETENTION AGES AT THE INSIGHT AND SPIRIT LANDING SITES. S. A. Wilson[1], N. H. Warner[2], J. A. Grant[1], M. P. Golombek[3], C. M. Weitz[4], [1] Center for Earth and Planetary Studies, National Air and Space Museum, Smithsonian Institution, 6th at Independence SW, Washington, DC, 20560 (wilsons@si.edu), [2]SUNY Geneseo, Department of Geological Sciences, 1 College Circle, Geneseo, NY 14454, [3]Jet Propulsion Laboratory, California Institute of Technology, Pasadena, CA, [4]Planetary Science Institute, 1700 East Fort Lowell, Tucson, AZ, 85719.

Introduction: The *InSight* mission landed in a ~27 m-diameter (D) degraded crater informally named *Homestead hollow* in Elysium Planitia [e.g., 1-3]. Elysium is characterized by smooth, basaltic lava plains estimated to be Hesperian (based on the size frequency distribution (SFD) of craters with D > 5 km) to Early Amazonian in age (based on the SFD of craters between 200m and 1 km in diameter [e.g., 4]). Nearly 15 years prior to *InSight*'s arrival on Mars, the Mars Exploration Rover (MER) *Spirit* landed on Late Hesperian- to Amazonian-aged [e.g., 5-8] basaltic lava plains in Gusev crater. Along its traverse, the *Spirit* rover investigated sediment-filled hollows that are comparable in size and general appearance [e.g., 9-11] to *Homestead hollow*, yet many appear to retain better-preserved rims (e.g., less degraded).

The landing site for the *InSight* mission was selected during the Mars Reconnaissance Orbiter (MRO) era of high resolution orbital data. As a result, the final landing ellipse was covered with images from the MRO High Resolution Imaging Science Experiment (HiRISE) [12] with resolutions of ~0.25 m per pixel [13] and the MRO Context camera (CTX) [14] with resolutions of ~6 m per pixel. Previous work using HiRISE data established a crater classification system and degradational continuum (Class 1 are pristine craters, down to Class 7 which are the most degraded craterforms that can still be positively identified), constrained the degradation processes, and estimated crater degradation rates for relatively fresh, 10 to 100-m-scale craters across the entire final *InSight* landing ellipse [4]. Since landing in *Homestead hollow*, this line of inquiry was expanded to include additional degraded, hollow-like craters (Class 8) in the region of the *InSight* lander to provide context and help interpret geological observations at the lander scale [2].

Motivation: Despite the broad similarities between the *Spirit* and *InSight* landing sites, the craters at the *Spirit* landing site have not yet received the same analyses using MRO data. Using comparable datasets and techniques, we aim to understand if the populations of degraded craters and quasi-circular depressions on the floor of Gusev crater follow the same degradation continuum as observed at the *InSight* landing site. The comparison between Gusev and Elysium will further our understanding of the degradation history of craters on Hesperian- to Early Amazonian-aged volcanic surfaces and provides constraints on the timing and extent of burial and exhumation events.

Methods: Gusev crater statistics were compiled using CraterTools [15], a plug-in software for ArcGIS (v. 10.6). Craters, excluding obvious secondary clusters, were counted using CTX data in a ~2,500 square km region around the *Spirit* landing site. We also determined the SFD of craters using HiRISE data in a preliminary ~9 square km area north of the *Spirit* landing site (**Fig. 1**). Each crater in the HiRISE data is classified based on its observed state of degradation (Class 1-8 after [2, 4]). We plan to use comparable areas, datasets, and methodology in Gusev so that we can directly compare the results to the analyses done at the *InSight* landing site in Elysium Planitia [2]. Relative ages of the surfaces were interpreted from cumulative plots created in Craterstats software, using the Mars chronology function of [16], production function of [17], and the equilibrium function of [18] (**Fig. 2**)

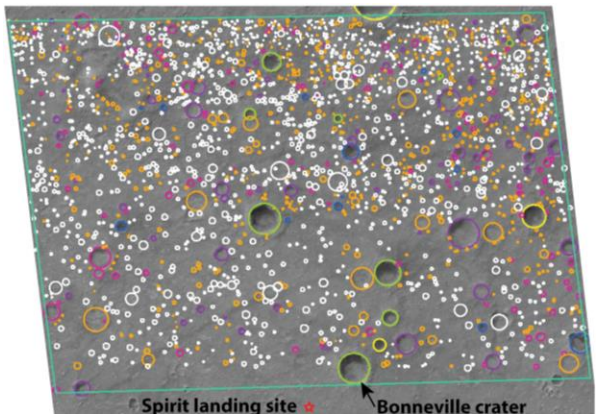

Figure 1. Preliminary map of craters classified in a ~ 9 km square area (green box) north of the MER *Spirit* landing site (red star). Craters are classified based on their observed state of degradation from Class 2 (more pristine) through Class 8 (hollows) after [2, 4]. Class 2 (yellow), Class 3 (e.g. Bonneville crater, green), Class 4 (blue), Class 5 (purple), Class 6 (pink), Class 7 (orange), Class 8 (white). Future work will extend the crater map to 21 square km (encompassing the *Spirit* landing site) to be consistent with previous work in Elysium [2]. Subframe of HiRISE ESP_025815_1655 (0.25 m/pixel) near -14.58°N, 175.48°E. North is up.

Preliminary Results and Observations: Morphologically distinct populations of craters are apparent on the Gusev plains, ranging from bowl shaped to quasi-circular depressions.

Observations from CTX data: In a ~2,500 square km area encompassing the volcanic plains in the vicinity of the *Spirit* landing site, a preliminary population of all craters between D~0.2-1 km is consistent with the expected population production function, yielding an Early Amazonian age (estimated absolute age is ~2.2 Ga, similar to the *InSight* landing site).

Observations from HiRISE data: The total number of craters counted in the preliminary crater map area of ~9 square km using HiRISE data (**Fig. 1**) is 2,431 (ranging in diameter from 3 to ~300 m). Class 8 has 1,527 craters, Class 7 has 674, Class 6 has 134, Class 5 has 68, Class 4 has 15, Class 3 has 10, and Class 2 has 3 craters. Only 29 craters are ≥ 100 m in diameter and 6 are ≥ 200 m in diameter. The crater mapping in Elysium in a 21 square km area resulted in just over 2,000 craters [2], implying that the Gusev plains may retain smaller craters more efficiently relative to the *InSight* landing site.

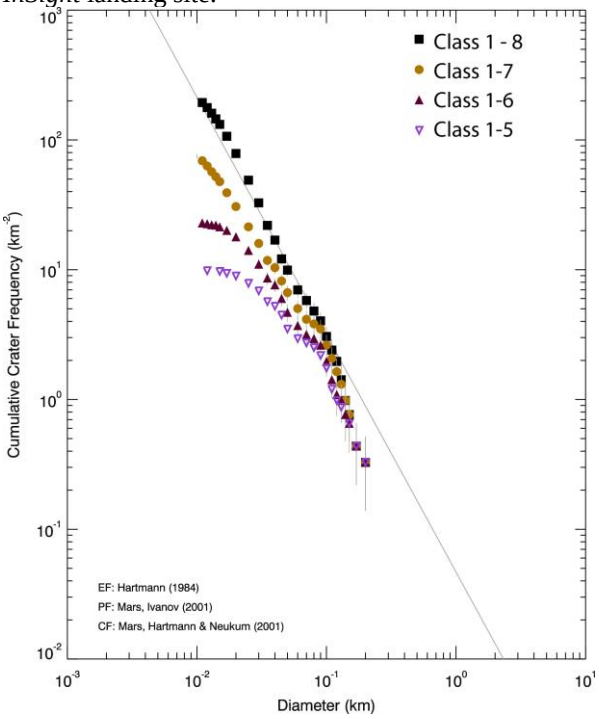

Figure 2. Cumulative size frequency histogram showing the distribution for Class 1-5 (purple triangles), 1-6 (red triangles), 1-7 (orange circles), and 1-8 (black squares) craters (see Fig. 1 for context). The approximate absolute age of the surface is ~1.6-1.8 Ga based craters with diameters between 90m – 250m that provide the best fit to the production function.

The cumulative SFD plots for craters in Class 1 to 5, 1 to 6, 1 to 7, and 1 to 8 are shown in **Figure 2**. As seen at the *InSight* landing site, the size frequency distribution of the Class 8 hollows points to an impact origin [2], and craters with diameters less than 100 m generally follows the -2 slope that is similar to the equilibrium function of [17]. The D ≤ 100 m-scale population of relatively pristine craters, however, falls below the equilibrium line (most pronounced for Class 1-5 craters). Similar to Elysium, this observation points to non-linear degradation rates over time, whereby early degradation was followed by much slower degradation [2-3]. The lower slope of the SFD for craters <100m is shallower than the expected production function or the equilibrium function, suggesting smaller craters are eroding faster than larger craters (consistent with hollows measured from the rover and from Mars Orbiter Camera data [10]). The kink in the SFD of craters near 100 m diameter is consistent with a resurfacing event around 200-300 Ma (based on craters 40 to 70 m in diameter). Similarities in crater populations and erosion rates at two different localities on Mars highlights the relative importance of geomorphic processes responsible for degrading volcanic plains for the past ~1 Ga.

References: [**1**] Golombek et al. (2020), *Nature Comm, in review.* [**2**] Warner, N. H., et al. (2020), An impact crater origin for Homestead hollow, the *InSight* landing site on Mars, 51st *LPSC*. [**3**] Grant, J. A. et al. (2020), The origin of rocky field at the *InSight* landing site in Homestead hollow and implications for the timing of degradation, 51st *LPSC*. [**4**] Sweeney, J., et. al (2018), *JGR* 123, 2732–2759, https://doi.org/10.1029/ 2018JE0 05618 [**5**] Cabrol, N. A., et al. (1998), *Icarus*, 98–108. [**6**] Cabrol, N. A., et al., (1998), *JGR*, 108(E12), 8076, doi:10.1029/2002JE002026. [**7**] Kuzmin, R. O., et al. (2000), Geologic Inv. Series, 8, pp., USGS Reston, Va.. [**8**] Milam, K. A., et al., (2003), *JGR*, 108 (E12), 8078, doi:10.1029/2002JE00 2023. [**9**] Grant et al. (2006), *JGR*, doi:10.1029/2005J E002465. [**10**] Golombek, M. P., et al. (2006), *JGR*, doi:10.1029/200 5JE002503. [**11**] Weitz et al. (2019), AGU, Abstract D151B-0022. [**12**] McEwen et al. (2007), *JGR*, 112, E05S02, doi:10.1029/2005JE00 2605. [**13**] Golombek et al. (2017), *Space Sci Rev* (2017) 211: 5. https://doi.org/10.1007/s11214-016-0321-9. [**14**] Malin et al. (2007), *JGR*., 112, E05S04, doi:10.1029/ 2006JE002808. [**15**] Kneissl, T., et al. (2011), *Planet. Space Sci*., 59, 1243-1254. [**16**] Hartmann, W. K., G. Neukum (2001), *Space Sci. Rev*., 96 (1–4), 165–194, doi:10.1023/A:10119452220. [**17**] Ivanov, B.A. (2001), *Space Sci. Rev*., 96(1–4), 87–104, doi:10.1023/A:1011941121102. [**18**] Hartmann, W. K. (1984), *Icarus*, 60, 56–74.